

## Protective Effect of Esculin on Streptozotocin-Induced Diabetic Renal Damage in Mice

Ki Sung Kang,<sup>\*,†,‡</sup> Woojung Lee,<sup>†</sup> Yujung Jung,<sup>†</sup> Ji Hwan Lee,<sup>†</sup> Seungyong Lee,<sup>†</sup> Dae-Woon Eom,<sup>§</sup> Youngsic Jeon,<sup>†</sup> Hye Hyun Yoo,<sup>||</sup> Ming Ji Jin,<sup>||</sup> Kyung Il Song,<sup>⊥</sup> Won Jun Kim,<sup>⊥</sup> Jungyeob Ham,<sup>†</sup> Hyoung Ja Kim,<sup>#</sup> and Su-Nam Kim<sup>\*,†</sup>

<sup>†</sup>Natural Medicine Center, Korea Institute of Science and Technology, Gangneung 210-340, Korea

<sup>‡</sup>College of Korean Medicine, Gachon University, Seongnam 461-701, Korea

<sup>§</sup>Department of Pathology, University of Ulsan College of Medicine, Gangneung 210-711, Korea

<sup>||</sup>Institute of Pharmaceutical Science and Technology and College of Pharmacy, Hanyang University, Ansan, Gyeonggi-do 426-791, Korea

<sup>⊥</sup>Department of Internal Medicine, College of Medicine and Gangneung Asan Hospital at University of Ulsan, Gangneung 210-711, Korea

<sup>#</sup>Molecular Recognition Research Center, Korea Institute of Science and Technology, Seoul 136-791, Korea

### **S** Supporting Information

**ABSTRACT:** The present study investigated the presence and mechanism of esculin-mediated renoprotection to assess its therapeutic potential. Esculin was orally administered at 20 mg/kg/day for 2 weeks to streptozotocin-induced diabetic mice, and its effects were compared with those of the vehicle in normal and diabetic mice. After oral administration of esculin to mice, the concentrations of esculin and esculetin in blood were  $159.5 \pm 29.8$  and  $9.7 \pm 4.9$  ng/mL at 30 min, respectively. Food and water intake were significantly increased in the diabetic mice compared to normal mice but attenuated in mice receiving esculin. The elevated blood glucose level and hepatic glucose-6-phosphatase expression were significantly reduced in esculin-treated diabetic mice, supporting the antidiabetic effect of esculin. Esculin also increased the uptake of glucose and induced the insulin-evoked phosphorylation of insulin receptor, Akt, and glycogen synthase kinase  $3\beta$  in C2C12 myotubes, indicating a potential for improvement of insulin sensitivity. In addition, esculin lessened the elevated blood creatinine levels in diabetic mice and ameliorated diabetes-induced renal dysfunction by reducing caspase-3 activation in the kidney. Data support the beneficial effect of esculin against diabetes and oxidative stress-related inflammatory processes in the kidney.

**KEYWORDS:** ash bark, esculin, diabetes, renal damage, caspase-3

## ■ INTRODUCTION

Diabetes mellitus is characterized by hyperglycemia and is a major cause of mortality and morbidity worldwide. An abnormally elevated blood glucose level causes oxidative stress and formation of advanced glycation end products, which have been closely linked to diabetic complications.<sup>1,2</sup> In particular, diabetics are at increased risk for several types of kidney disease, and the predominant cause of end-stage renal disease in this disorder is diabetic nephropathy.<sup>3</sup> Prevention and treatment of diabetic nephropathy have become an important issue.

Many attempts have been made to improve the treatment of diabetes. Although various kinds of hypoglycemic drugs are available for the control of hyperglycemia, there is no satisfactory medical therapy that does not produce undesirable side effects.<sup>4</sup> Chemical and pharmacological research studies have identified numerous bioactive and nontoxic compounds in naturally occurring nutraceuticals and botanical drugs in efforts to find novel therapeutic agents for treatment of diabetic nephropathy.<sup>5–7</sup>

Coumarins comprise a large class of natural phenolic substances found in various plants and are constituted of fused benzene and  $\alpha$ -pyrone rings. This class of compounds

influences the formation and scavenging of reactive oxygen species (ROS) and processes involving free radical-mediated damage.<sup>8,9</sup> Coumarins vary widely in structure due to the types of substitutions in their basic rings, which can influence their biological activity.<sup>10–12</sup> Esculin is a coumarin derivative that has been demonstrated to have multiple biological functions including intestinal anti-inflammatory activity,<sup>12</sup> antioxidant activity,<sup>13</sup> and anticancer activity including growth inhibition of human leukemia cells.<sup>14,15</sup> In addition, diabetes-related *in vitro* studies showed that esculin and its metabolite esculetin inhibit formation of advanced glycation end-products formation and the activities of  $\alpha$ -glucosidase and protein tyrosine phosphatase 1B.<sup>16,17</sup>

Investigation of specific bioactive constituents is important for identification of the precise mechanisms of action and development of therapeutic herbal remedies.<sup>7</sup> However, studies on the effect and mechanism of esculin (Figure 1A) on diabetic

**Received:** May 24, 2013

**Revised:** January 23, 2014

**Accepted:** January 31, 2014

**Published:** January 31, 2014

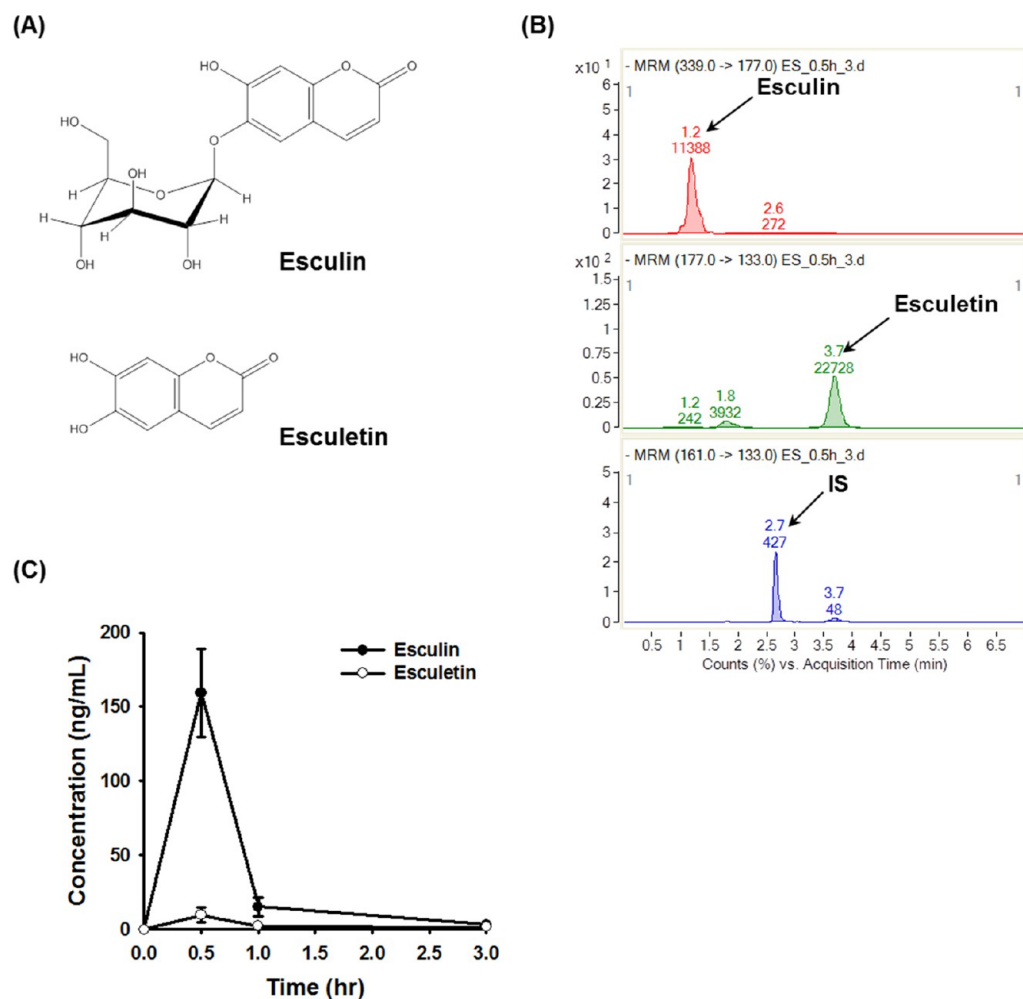


**Figure 1.** Blood levels of esculin and esculletin after oral administration of esculin in mice. (A) Structures of esculin and esculletin. (B) Representative MRM chromatograms for plasma samples collected after administration of esculin. (C) Blood concentrations of esculin and esculletin in mice.

renal damage are limited. To address this shortcoming, we investigated the effect of esculin, a major active component of ash bark, on glucose metabolism, oxidative stress, and inflammation in diabetic-damaged kidney to identify its effects and mechanism of action in diabetes. Furthermore, the pharmacokinetics of esculin and its metabolite esculletin were simultaneously examined in plasma samples from mice by liquid chromatography-electrospray ionization-tandem mass spectrometry.

## MATERIALS AND METHODS

**Chemicals.** Streptozotocin (STZ), esculin, and esculletin (purity 98–100%) were purchased from Sigma Aldrich (Seoul, South Korea). Antibodies for Akt, phosphor-Ser473 Akt (pS473-Akt), insulin receptor  $\beta$  (IR $\beta$ ), phosphor-IR $\beta$  at Tyr1150/1151 (pY1150/51-IR), glycogen synthase kinase 3 $\beta$  (Gsk3 $\beta$ ), phosphor-Ser9-Gsk3 $\beta$  (pS9-Gsk3 $\beta$ ), glyceraldehyde 3-phosphate dehydrogenase (GAPDH), cleaved caspase-3,  $\beta$ -actin, and horseradish peroxidase (HRP) conjugated antirabbit antibodies were purchased from Cell Signaling (Boston, MA, USA). Other chemicals and reagents used were of high quality and obtained from commercial sources.

**Cell Culture.** C2C12 mouse myoblast cell line was obtained from ATCC and cultured in Dulbecco's modified Eagle's medium (DMEM; Invitrogen, Carlsbad, CA, USA) supplemented with 10% fetal bovine serum (FBS; HyClone Laboratories, Logan, UT, USA) and 1% penicillin/streptomycin (Invitrogen) at 37 °C with 5% CO<sub>2</sub> in air.

**Myotube Formation and Immunoblotting.** C2C12 myoblast were cultured in DMEM until 90% of confluence. Cells were differentiated into myotubes with DMEM containing 2% horse serum for 4 days and then incubated for 16 h in DMEM containing 2% BSA and 10% FBS in the absence or presence of esculin. Subsequently, the esculin-treated cells were stimulated with 100 nM insulin for 10 min. After stimulation, cells were washed twice with PBS and harvested. For Western blotting, antibodies for Akt, phosphor-Ser473 Akt (pS473-Akt), insulin receptor  $\beta$  (IR $\beta$ ), phosphor-IR $\beta$  Tyr1135/1136 IGF-1 R $\beta$  /Tyr1150/1151, Gsk3 $\beta$  phosphor-Ser9-Gsk3 $\beta$ , and GAPDH were used.

**2-[N-(7-Nitrobenz-2-oxa-1,3-diazol-4-yl)amino]-2-deoxy-D-glucose (2-NBDG) Glucose Uptake Assay.** The myotubes, which were obtained from the above procedures, were stimulated with 100 nM insulin for 1 h. After insulin stimulation, the myotubes were incubated with 50  $\mu$ M 2-NBDG (Invitrogen) for 15 min and then washed with PBS three times to remove free 2-NBDG. The fluorescence intensity of cells containing 2-NBDG was measured on the Infinite M1000 microplate reader (TECKAN) with excitation at 485 nm and emission at 535 nm.

**Animal Experiments.** The Guidelines for Animal Experimentation, approved by the Korea Institute of Science and Technology, were followed in these experiments. Male ICR mice weighing 30–35 g were used for evaluating the protection of the esculin against STZ-induced diabetic renal damage. The mice were housed under temperature (23  $\pm$  2 °C) and humidity (55  $\pm$  5%) conditions with a standard light (12 h light/dark). The mice were given free access to water and a normal diet (38057, Agribands Purina Korea, Seongnam, Gyeonggi, Korea)

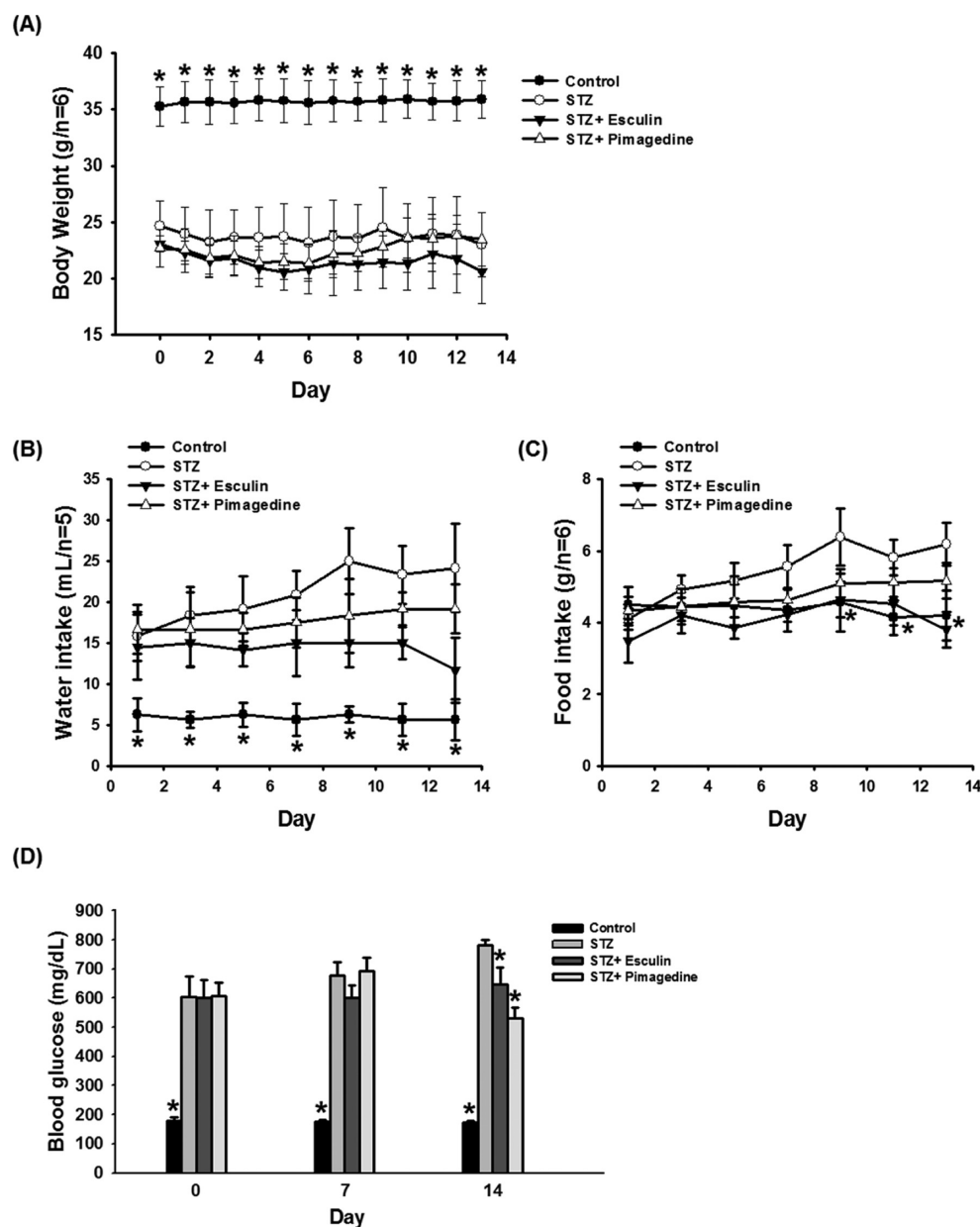


**Figure 2.** Effects of esculin on physiological parameters in the STZ-induced diabetes model. (A) Changes in body weight. (B) Changes in water intake. (C) Changes in food intake. (D) Changes in blood glucose levels.  $p < 0.05$  compared to the STZ-treated control value.

containing 10 kcal % fat for a period of 1 week after arrival. After several days of adaptation, STZ dissolved in citrate buffer (10 mM, pH 4.5) was injected intraperitoneally at a dose of 200 mg/kg body weight following overnight fasting. The mice underwent a sham injection of citrate buffer without STZ and were also used as normal group ( $n = 5$ ). The blood glucose level was determined, and the body weight was measured after 7 days of STZ injection, and to avoid any intergroup differences in these indices, the diabetic mice were divided into three experimental groups: group 1, diabetic mice received water (diabetic control,  $n = 6$ ); groups 2, diabetic mice received 20 mg/kg body weight/day of esculin orally via gavage once a day (diabetic + esculin,  $n = 6$ ); and group 3, diabetic mice received 20 mg/kg body weight/day of pimagedine orally via gavage once a day (diabetic + pimagedine,  $n = 6$ ). The 20 mg/kg of esculin dosage was chosen according to the literature<sup>18</sup> and preliminary experiments. The mice were sacrificed 14 days after sample administration under light ether anesthesia. Blood samples were collected from abdominal aorta, and the serum was separated immediately from the blood samples by centrifugation. Kidneys and livers were removed, quickly frozen, and kept at  $-80^{\circ}\text{C}$

until analysis. All preparations and analyses of various parameters were performed simultaneously under similar experimental conditions to avoid any day to day variations.

Another abbreviated experiment to compare the blood levels of esculin and esculetin at three selected time points (0.5, 1, and 3 h) in mice ( $n = 4$ ) was also conducted. Blood samples were collected from abdominal aorta under light ether anesthesia at 0.5, 1, and 3 h after esculin oral administration (20 mg/kg). The mice were sacrificed in each time point. About 500  $\mu\text{L}$  blood was drawn and collected in a heparin-coated tube, and plasma was obtained following rapid centrifugation and immediately frozen at  $-80^{\circ}\text{C}$  until analysis.

**LC/MS/MS Analyses for Esculin and Esculetin in Blood.** Plasma samples were analyzed for esculin and esculetin using the LC/MS/MS method reported previously.<sup>19</sup> The LC/MS/MS system consisted of an Agilent 1260 Infinity high-performance liquid chromatography (HPLC) system with an Agilent 6460 triple-quadrupole mass spectrometer (Agilent Technologies, Palo Alto, CA) equipped with a turbo ion spray source. Chromatographic separation was achieved with a BDS Hypersil C<sub>18</sub> column (50 mm

×2.1 mm ID, 5  $\mu$ L, Thermo Fisher Scientific Inc., Waltham, MA), and oven temperature was maintained at 40 °C. The mobile phase consisted of 0.1% formic acid (solvent A) and 90% acetonitrile with 0.1% formic acid (solvent B). A gradient program was used for HPLC separation, with a flow rate of 0.25 mL/min the gradient program began with 10% B, which was increased to 90% in 1 min, was maintained to 4 min, and followed by 4 min re-equilibration. Electrospray ionization was performed in negative ion mode. The precursor–product ion pairs monitored in multiple reaction monitoring (MRM) detection were 339→177 for esculin, 177→133 for esculetin, and 161→133 for 7-OH-coumarin (IS). The representative MRM chromatograms are shown in Figure 1B. Calibration curves for analytes were obtained using 9 points in the range 1–500 ng/mL. Calibration curves were generated by plotting the peak area ratio for esculin or esculetin to IS versus the concentration of esculin or esculetin in the standard-spiked plasma by least-squares linear regression. The calibration curve equations are  $y = 0.1215x - 0.0368$  ( $r^2 = 0.999$ ) for esculin and  $y = 0.0747x - 0.0058$  ( $r^2 = 0.999$ ) for esculetin.

**Histological Examination.** After fixation of the kidneys with 10% formalin, renal tissues were sectioned and stained with hematoxylin and eosin (HE) reagents for histological examination. Tubular damage in HE-stained sections was examined under the microscope and scored based on the percentage of cortical tubules showing epithelial necrosis: 0, normal; 1, <10%; 2, 10–25%; 3, 26–75%; 4, >75%. Tubular necrosis was defined as tubular epithelial degeneration, interstitial inflammation, and architectural abnormality as described previously.<sup>20</sup> The morphometric examination was performed in a blinded manner by two independent investigators.

**Western Blot Analysis.** Frozen kidney tissues were homogenized with a lysis buffer (contents of 1% NP-40, 20 mM Tris-HCl, 150 mM NaCl, 1 mM Na<sub>2</sub>EDTA, 1 mM EGTA, 1% sodium deoxycholate, and 100 mM PMSF) and centrifuged at 13 000 rpm at 4 °C for 20 min to obtain the cellular proteins in the supernatant. Differential protein expression patterns were assessed by Western blot following protein quantification by the Lowry and Bradford methods. Equal amounts of proteins from each sample were resolved by SDS-PAGE, transferred to polyvinylidene fluoride (PVDF) membranes for 1 h at semidry, and blocked in blocking buffer for 1 h at room temperature. PVDF membranes were incubated with primary antibody against cleaved caspase-3 (1:1000 dilution),  $\beta$ -actin (1:1000 dilution) overnight at 4 °C, washed three times for 5 min to wash buffer, incubated with HRP-conjugated secondary antibody (1:2000 dilution, antirabbit) for 1 h at room temperature, washed three times, and then detected with ECL solution.

**Gene Expression Analysis.** Total RNA was isolated from tissue using the TRIzol reagent (Invitrogen, Carlsbad, CA) according to the manufacturer's instructions. The RNA concentration of each sample was determined by spectrophotometry at 260 nm; the integrity of each RNA sample was evaluated using the Agilent 2100 BioAnalyzer (Agilent Technologies, Santa Clara, CA). cDNA synthesis was performed using 1  $\mu$ g of total RNA in 20  $\mu$ L with random primers and Superscript II reverse transcriptase. Quantitative real-time PCR (Q-PCR) analyses were performed with SYBR green fluorescent dye using the 7500 Real-Time PCR System (Applied Biosystem, Foster City, CA). Data analyses were performed using 7500 System SDS software version 1.3.1 (Applied Biosystem). Primer sets used in this study were as follows: glucose 6-phosphatase (G6 Pase), forward 5'-ATGACTTTGGGATCCAGTCG-3' and reverse 5'-TGGAACCA-GATGGGAAAGAG-3' and glyceraldehyde-3-phosphate dehydrogenase (GAPDH), forward 5'-TTGTTGCCATCAACGACCCC-3' and reverse 5'-GCCGTTGAATTTGCCGTGAG-3'.

**Statistical Analysis.** Statistical significance was determined through analysis of variance (ANOVA) followed by a multiple comparison test with a Bonferroni adjustment. *P* values of less than 0.05 were considered statistically significant.

## RESULTS

**Blood Levels of Esculin and Esculetin after Oral Administration of Esculin in Mice.** After oral administration of esculin to mice (20 mg/kg body weight), there was a rapid and short-lasting increase in plasma esculin and esculetin levels. The concentrations of esculin and esculetin in blood were  $159.5 \pm 29.8$  and  $9.7 \pm 4.9$  ng/mL at 30 min, respectively (Figure 1C). Although a large portion of esculin was detected in the blood, esculetin, which is a deglycosylated metabolite of esculin, was also detected (Figure 1C).

**Antidiabetic Effect and Mechanism of Esculin Against STZ-Induced Type 1 Diabetes in Mice.** Figure 2 shows the effects of esculin on the changes in physico-metabolic symptoms with diabetes over the 14-day experimental period. The body weight of mice after STZ and STZ + esculin or pimaginedine was markedly reduced compared to that of control mice (Figure 2A). In comparison, the intake of water and food were significantly increased in the STZ-treated mice (Figure 2B and 2C). Although no significant amelioration was evident, oral administration of esculin or pimaginedine at a dose of 20 mg/kg for 14 days attenuated the diabetes-induced physiological abnormalities. The blood glucose level of diabetic mice was markedly higher than that of normal mice, and it was continuously increased during the experimental period. The elevated glucose level was significantly reduced in diabetic mice given 20 mg/kg esculin or pimaginedine (Figure 2D).

As shown in Figure 3A, the plasma alanine aminotransferase (ALT) levels of diabetic mice were significantly increased more than those of normal control mice. However, treatment with esculin led to a significant decrease in plasma ALT levels (Figure 3A). The expression level of G6 Pase gene expression in the liver was significantly increased in diabetic animals. The elevated expression level of G6 Pase was markedly reduced in esculin-treated diabetic mice (Figure 3B), supporting the antidiabetic effects of esculin; however, the effect of esculin was weaker than that of pimaginedine (Figure 3B).

**Effect of Esculin on Insulin Sensitivity.** To ascertain the positive effects of esculin on insulin sensitivity, we first examined glucose uptake in C2C12 myotubes under normal conditions. As shown in Figure 4A, glucose uptake in C2C12 myotubes in the absence or presence of insulin was significantly enhanced by esculin treatment under normal conditions. Correspondingly, esculin (50  $\mu$ M) application also enhanced the insulin-evoked phosphorylation of IR, Akt, and GSK-3 $\beta$  under normal conditions, indicating a potential for improvement of insulin sensitivity (Figure 4B).

**Renoprotective Effect of Esculin Against STZ-Induced Diabetic Renal Damage in Mice.** The elevated serum creatinine level of STZ-treated mice was significantly reduced by esculin (Figure 5A). HE staining was performed on renal sections to measure tubular damage. As shown in the representative pictures of renal sections, severe tubulointerstitial injuries including tubular epithelial cell detachments, cystic dilatation of tubules, and inflammatory cell infiltration occurred in kidneys of STZ-treated diabetic mice (Figure 5B). However, the increased tubular damage in STZ-treated mice was reduced by treatment with esculin (Figure 5B). Figure 6A shows the effect of esculin on the cleaved caspase-3 protein expression in STZ-treated mice kidneys. The cleaved caspase-3 protein expression was significantly increased after STZ injection, and cotreatment with esculin afforded significant renoprotection (Figure 6B).



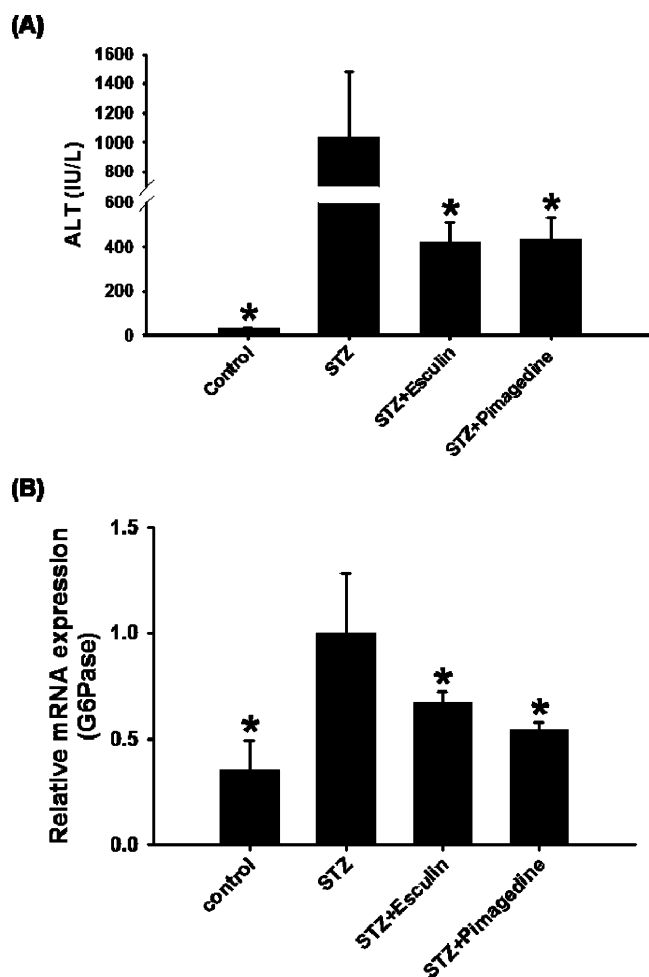


**Figure 3.** Effects of esculin on serum ALT and hepatic glucose 6-phosphatase levels in the STZ-induced diabetes model. (A) Serum ALT levels. (B) Hepatic glucose 6-phosphatase levels.  $p < 0.05$  compared to the STZ-treated control value.

## DISCUSSION

Many diabetic patients choose complementary and alternative therapies along with mainstream antidiabetic drugs, which has increased demand for alternative therapies for diabetes.<sup>21</sup> In the present study, we investigated the antidiabetic effect and mechanism of esculin, an active ingredient of ash bark, on kidney damage caused by hyperglycemia, oxidative stress, and inflammation to evaluate its possible use in treatment of diabetic renal damage.

To evaluate the effect of esculin on diabetic renal damage, we administered esculin to STZ-induced diabetic mice and monitored plasma glucose levels in each animals. After oral administration of esculin to mice, there was a rapid and short-lasting increase in plasma esculin and esculetin levels. Over the experimental period, the levels of water and food intake were significantly elevated in diabetic mice, indicating the changes in physiological changes that result from the increased blood glucose levels. STZ enters the  $\beta$  cell via a glucose transporter (GLUT2) and liberates toxic amounts of free radicals that cause damage to the DNA. Oxidative inflammation is implicated in pancreatic  $\beta$ -cell injury, leading to development of diabetes mellitus.<sup>22</sup> The pancreatic islet size and blood insulin levels of diabetic mice was markedly lowered than those of normal control mice, but there were no significant ameliorations in islet

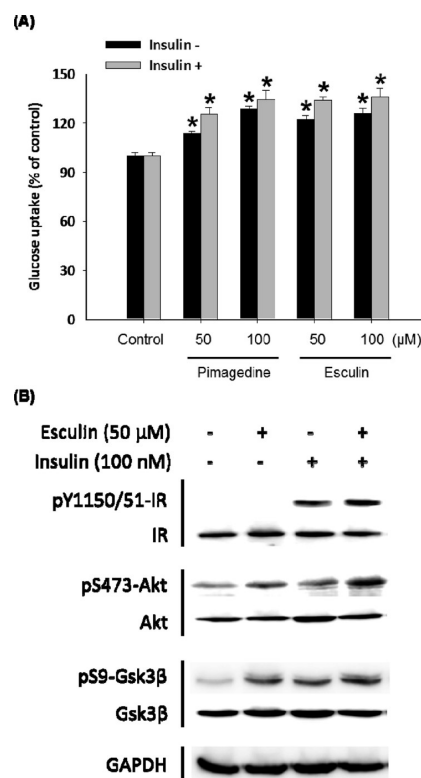


**Figure 4.** Effects of esculin on glucose uptake and insulin sensitivity in C2C12 myotubes. (A) Basal and insulin-stimulated glucose uptake in pimagedine and esculin-treated C2C12 myotubes under normal conditions. (B) Level of phosphorylation of IR, Akt, and GSK-3 $\beta$  in esculin-treated C2C12 myotubes under normal conditions. Protein levels were analyzed by Western blot.  $p < 0.05$  compared to the control value.

size or blood insulin levels after esculin treatments (Supplemental Figure 1, Supporting Information). Therefore, the beneficial effect of esculin on blood glucose might be related to other factors than pancreatic damage by STZ. Because hepatic gluconeogenesis gene expression is markedly increased in diabetic animals and contributes to hyperglycemia, expression of G6 Pase, one of the key enzymes in gluconeogenesis,<sup>23</sup> was measured in the liver tissue of diabetic mice. The expression level of G6 Pase was significantly reduced in esculin-treated mice, supporting the antidiabetic effect of esculin.

The tyrosine phosphorylation of IR $\beta$  subunit is necessary for insulin signal transduction into the cells. In particular, phosphorylation of tyrosine 1146, 1150, and 1151 is crucial for activation of the IR which initiates further downstream signaling events.<sup>24</sup> Akt regulates glycogen synthesis through phosphorylation within the carboxy terminus at Ser473 and inactivation of GSK-3 $\alpha$  and  $\beta$ , which was initially identified as an enzyme that regulates glycogen synthesis in response to insulin.<sup>25</sup> In the present study, esculin increased the uptake of glucose and induced the insulin-evoked phosphorylation of IR $\beta$ , Akt, and glycogen synthase kinase 3 $\beta$  in C2C12 myotubes, indicating a potential for improvement of insulin sensitivity.

Hyperglycemia-induced abnormal production of ROS has been implicated in the etiology of diabetic nephropathy, with ROS having critical roles in the development and progression of kidney damage.<sup>26–28</sup> In patients with diabetes and/or renal failure, the level of blood creatinine, which is an effective index for expressing the glomerular filtration rate, increases

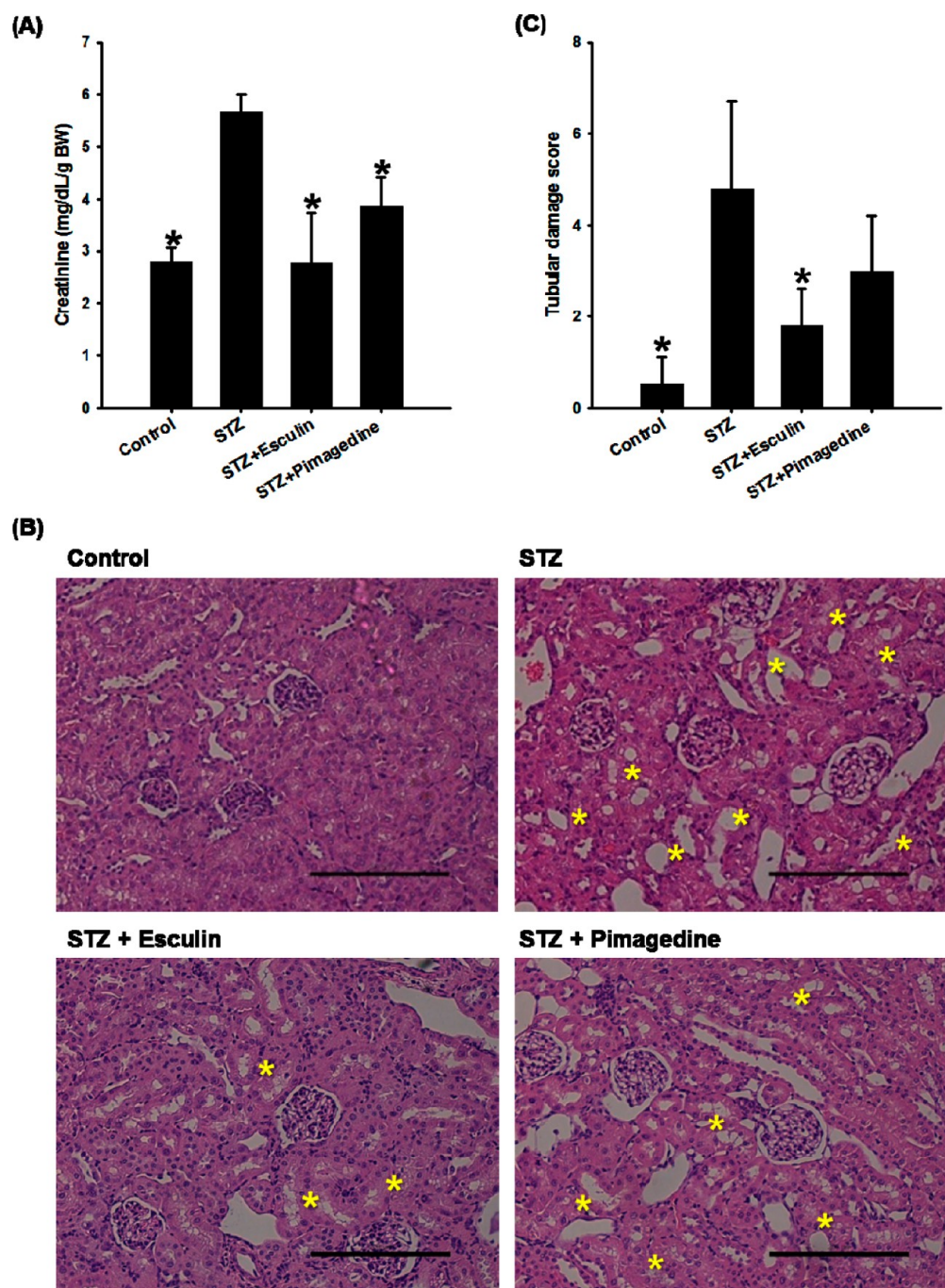


**Figure 5.** Effects of esculin on renal function and histopathological changes in the STZ-induced diabetes model. (A) Serum creatinine levels. (B) HE staining of representative renal section. (C) Tubular damage score. Yellow asterisks indicate tubular damage.  $p < 0.05$  compared to the STZ-treated control value.

exponentially and eventually causes nephritic syndrome.<sup>29</sup> However, the present investigation showed that administration of esculin or pimagedine for 14 days significantly reduced the levels of blood creatinine. Therefore, the diabetic renal dysfunctions of diabetic mice were improved by the administration of esculin.

STZ activates various pro-inflammatory and apoptotic molecules including the caspase-3 and Bax systems.<sup>30–32</sup> Synthetic or naturally occurring caspase inhibitors have the potential to minimize uncontrolled apoptosis in STZ-induced nephropathy.<sup>31,33</sup> For example, the antioxidant compound alpha-lipoic acid can abrogate the oxidative stress induced in

mesangial cells and rat kidney by elevated glucose levels.<sup>30</sup> Our results also showed significant increases in cleaved caspase-3 in the kidneys of diabetic mice; the elevated level was significantly reduced after esculin administration. These results imply that esculin may alleviate oxidative stress by preventing caspase-3 activation and related inflammation in the kidney.

Clinical evidence has suggested that the appropriate use of nutraceuticals or herbal medicines can prevent or ameliorate development of diabetic complications.<sup>34,35</sup> However, these medicines usually have an insufficient scientific basis and the exact mechanisms behind their beneficial effects are unknown. This study demonstrates that esculin ameliorates diabetes-

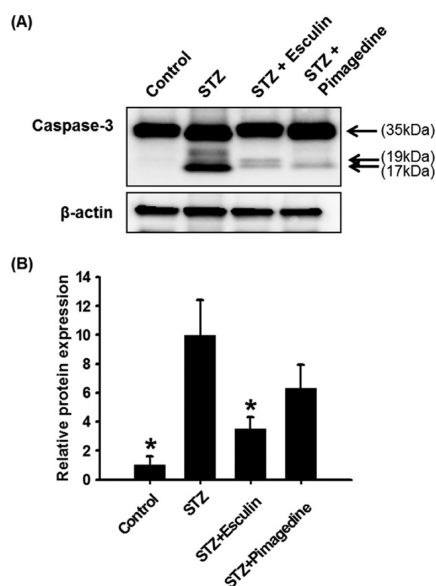


**Figure 6.** Effects of esculin on renal caspase-3 activation in the STZ-induced diabetes model. (A) Cleaved caspase-3 protein expression and (B) its quantitative data for Western blot analysis of renal cortex tissues.  $p < 0.05$  compared to the STZ-treated control value.

induced renal dysfunction by reducing the activation of caspase-3 in the kidney. The current experimental results provide therapeutic evidence of the renoprotective effects of esculin both in vitro and in vivo.

## ■ ASSOCIATED CONTENT

### 📄 Supporting Information

This material is available free of charge via the Internet at <http://pubs.acs.org>.

## ■ AUTHOR INFORMATION

### Corresponding Authors

\*Phone: 82-33-650-3512. Fax: 82-33-650-3028. E-mail: [kkang@kist.re.kr](mailto:kkang@kist.re.kr).

\*Phone: 82-33-650-3503. Fax: 82-33-650-3028. E-mail: [snkim@kist.re.kr](mailto:snkim@kist.re.kr).

### Funding

This work was funded by the Korea Institute of Science and Technology institutional program (2Z04210).

### Notes

The authors declare no competing financial interest.

## ■ REFERENCES

- (1) Ahmed, N. Advanced glycation endproducts-role in pathology of diabetic complications. *Diabetes Res. Clin. Pract.* **2005**, *67*, 3–21.
- (2) Baynes, J. W. Role of oxidative stress in development of complications in diabetes. *Diabetes* **1991**, *40*, 405–412.
- (3) Selby, J. V.; FitzSimmons, S. C.; Newman, J. M.; Katz, P. P.; Sepe, S.; Showstack, J. The natural history and epidemiology of diabetic nephropathy. Implications for prevention and control. *JAMA* **1990**, *263*, 1954–1960.
- (4) The Diabetes Control and Complications Trial Research Group. The effect of intensive treatment of diabetes on the development and progression of long-term complications in insulin-dependent diabetes mellitus. *N. Engl. J. Med.* **1993**, *329*, 977–986.
- (5) Yamabe, N.; Yokozawa, T.; Oya, T.; Kim, M. Therapeutic potential of (-)-epigallocatechin 3-O-gallate on renal damage in diabetic nephropathy model mice. *J. Pharmacol. Exp. Ther.* **2006**, *319*, 228–236.

(6) Kim, H. Y.; Kang, K. S.; Yamabe, N.; Nagai, R.; Yokozawa, T. Protective effect of heat-processed American ginseng against diabetic renal damage in rats. *J. Agric. Food Chem.* **2007**, *55*, 8491–8497.

(7) Rao, A. V.; Snyder, D. M. Raspberries and human health: a review. *J. Agric. Food Chem.* **2010**, *58*, 3871–3883.

(8) Paya, M.; Halliwell, B.; Hoult, J. R. S. Interactions of a series of coumarins with reactive oxygen species. Scavenging of superoxide, hypochlorous acid and hydroxyl radicals. *Biochem. Pharmacol.* **1999**, *44*, 205–214.

(9) Lin, W. L.; Wang, C. J.; Tsai, Y. Y.; Liu, C. L.; Hwang, J. M.; Tseng, T. H. Inhibitory effect of esculin on oxidative damage induced by t-butyl hydroperoxide in rat liver. *Arch. Toxicol.* **2000**, *74*, 467–472.

(10) Kostova, I. Synthetic and natural coumarins as cytotoxic agents. *Curr. Med. Chem.* **2005**, *5*, 29–46.

(11) Riveiro, M. E.; Moglioni, A.; Vazquez, R.; Gomez, N.; Facorro, G.; Piehl, L.; de Celis, E. R.; Shayo, C.; Davio, C. Structural insights into hydroxycoumarin-induced apoptosis in U-937 cells. *Bioorg. Med. Chem.* **2008**, *16*, 2665–2675.

(12) Witaicenis, A.; Seito, L. N.; Stasi, L. C. Intestinal anti-inflammatory activity of esculin and 4-methylesculin in the trinitrobenzenesulphonic acid model of rat colitis. *Chem. Biol. Interact.* **2010**, *186*, 211–218.

(13) Lee, B. C.; Lee, S. Y.; Lee, H. J.; Sim, G. S.; Kim, J. H.; Kim, J. H.; Cho, Y. H.; Lee, D. H.; Pyo, H. B.; Choe, T. B.; Moon, D. C.; Yun, Y. P.; Hong, J. T. Anti-oxidative and photo-protective effects of coumarins isolated from *Fraxinus chinensis*. *Arch. Pharm. Res.* **2007**, *30*, 1293–1301.

(14) Park, C.; Jin, C. Y.; Kim, G. Y.; Choi, I. W.; Kwon, T. K.; Choi, B. T.; Lee, S. J.; Lee, W. H.; Choi, Y. H. Induction of apoptosis by esculin in human leukemia U937 cells through activation of JNK and ERK. *Toxicol. Appl. Pharmacol.* **2008**, *227*, 219–228.

(15) Wang, C. J.; Hsieh, Y. J.; Chu, C. Y.; Lin, Y. L.; Tseng, T. H. Inhibition of cell cycle progression in human leukemia HL-60 cells by esculin. *Cancer Lett.* **2002**, *183*, 163–168.

(16) Jung, H. A.; Park, J. J.; Islam, M. N.; Jin, S. E.; Min, B. S.; Lee, J. H.; Sohn, H. S.; Choi, J. S. Inhibitory activity of coumarins from *Artemisia capillaris* against advanced glycation endproduct formation. *Arch. Pharm. Res.* **2012**, *35*, 1021–1035.

(17) Nurul Islam, M.; Jung, H. A.; Sohn, H. S.; Kim, H. M.; Choi, J. S. Potent  $\alpha$ -glucosidase and protein tyrosine phosphatase 1B inhibitors from *Artemisia capillaris*. *Arch. Pharm. Res.* **2013**, *36*, 542–552.

(18) Li, J. M.; Zhang, X.; Wang, X.; Xie, Y. C.; Kong, L. D. Protective effects of cortex fraxini coumarines against oxonate-induced hyperuricemia and renal dysfunction in mice. *Eur. J. Pharmacol.* **2011**, *666*, 196–204.

(19) Li, Y. Y.; Song, Y. Y.; Liu, C. H.; Huang, X. T.; Zheng, X.; Li, N.; Xu, M. L.; Mi, S. Q.; Wang, N. S. Simultaneous determination of esculin and its metabolite esculin in rat plasma by LC-ESI-MS/MS and its application in pharmacokinetic study. *J. Chromatogr., B: Anal. Technol. Biomed. Life Sci.* **2012**, *907*, 27–33.

(20) Mukhopadhyay, P.; Rajesh, M.; Pan, H.; Patel, V.; Mukhopadhyay, B.; B tkai, S.; Gao, B.; Hask , G.; Pacher, P. Cannabinoid-2 receptor limits inflammation, oxidative/nitrosative stress, and cell death in nephropathy. *Free Radical Biol. Med.* **2010**, *48*, 457–467.

(21) Ceylan-Isik, A. F.; Fliethman, R. M.; Wold, L. E.; Ren, J. Herbal and traditional Chinese medicine for the treatment of cardiovascular complications in diabetes mellitus. *Curr. Diabetes Rev.* **2008**, *4*, 320–328.

(22) Yabaluri, N.; Bashyam, M. D. Hormonal regulation of gluconeogenic gene transcription in the liver. *J. Biosci.* **2010**, *35*, 473–484.

(23) Szkudelski, T. The mechanism of alloxan and streptozotocin action in B cells of the rat pancreas. *Physiol. Res.* **2001**, *50*, 537–546.

(24) Gonz lez-S nchez, J. L.; Serrano-R os, M. Molecular basis of insulin action. *Drug News Perspect.* **2007**, *20*, 527–531.

(25) Kaidanovich, O.; Eldar-Finkelman, H. The role of glycogen synthase kinase-3 in insulin resistance and type 2 diabetes. *Expert Opin. Ther. Targets* **2002**, *6*, 555–561.

(26) Li, J. M.; Shah, A. M. ROS generation by nonphagocytic NADPH oxidase: potential relevance in diabetic nephropathy. *J. Am. Soc. Nephrol.* **2003**, *14*, S221–S226.

(27) Forbes, J. M.; Coughlan, M. T.; Cooper, M. E. Oxidative stress as a major culprit in kidney disease in diabetes. *Diabetes* **2008**, *57*, 1446–1454.

(28) Heyman, S. N.; Rosen, S.; Rosenberger, C. A role for oxidative stress. *Contrib. Nephrol.* **2011**, *174*, 138–148.

(29) Bell, D. S. Diabetic nephropathy: changing concepts of pathogenesis and treatment. *Am. J. Med. Sci.* **1991**, *301*, 195–200.

(30) Singh, L. P.; Cheng, D. W.; Kowluru, R.; Levi, E.; Jiang, Y. Hexosamine induction of oxidative stress, hypertrophy and laminin expression in renal mesangial cells: effect of the anti-oxidant alpha-lipoic acid. *Cell Biochem. Funct.* **2007**, *25*, 537–550.

(31) Kuhad, A.; Sachdeva, A. K.; Chopra, K. Attenuation of renoinflammatory cascade in experimental model of diabetic nephropathy by sesamol. *J. Agric. Food Chem.* **2009**, *57*, 6123–6128.

(32) Jung, D. S.; Lee, S. H.; Kwak, S. J.; Li, J. J.; Kim, D. H.; Nam, B. Y.; Kang, H. Y.; Chang, T. I.; Park, J. T.; Han, S. H.; Yoo, T. H.; Kang, S. W. Apoptosis occurs differentially according to glomerular size in diabetic kidney disease. *Nephrol. Dial. Transplant.* **2012**, *27*, 259–266.

(33) Nakano, M.; Matsumoto, I.; Sawada, T.; Ansite, J.; Oberbroeckling, J.; Zhang, H. J.; Kirchhof, N.; Shearer, J.; Sutherland, D. E.; Hering, B. J. Caspase-3 inhibitor prevents apoptosis of human islets immediately after isolation and improves islet graft function. *Pancreas* **2004**, *29*, 104–109.

(34) Chao, M.; Zou, D.; Zhang, Y.; Chen, Y.; Wang, M.; Wu, H.; Ning, G.; Wang, W. Improving insulin resistance with traditional Chinese medicine in type 2 diabetic patients. *Endocrine* **2009**, *36*, 268–274.

(35) Omar, E. A.; Kam, A.; Alqahtani, A.; Li, K. M.; Razmovski-Naumovski, V.; Nammi, S.; Chan, K.; Roufogalis, B. D.; Li, G. Q. Herbal medicines and nutraceuticals for diabetic vascular complications: mechanisms of action and bioactive phytochemicals. *Curr. Pharm. Des.* **2010**, *16*, 3776–3807.